SESAME – AN EXPERIMENT OF THE ROSETTA LANDER PHILAE: OBJECTIVES AND GENERAL DESIGN

K. J. SEIDENSTICKER[1,*], D. MÖHLMANN[1,2], I. APATHY[3], W. SCHMIDT[4], K. THIEL[5], W. ARNOLD[6], H.-H. FISCHER[5], M. KRETSCHMER[1,8], D. MADLENER[1,9], A. PÉTER[3], R. TRAUTNER[7] and S. SCHIEKE[1,10]

[1]*DLR, Institute of Space Simulation, D-51170 Köln, Germany*
[2]*DLR, Institute of Planetary Research, D-12489 Berlin, Germany*
[3]*KFKI, Atomic Energy Research Institute, H-1525 Budapest, Hungary*
[4]*FMI, Space Research Division, FIN-00560 Helsinki, Finland*
[5]*University of Cologne, Dept. of Nuclear Chemistry, D-50674 Köln, Germany*
[6]*Fraunhofer-Institute for Non-Destructive Testing (IZFP), Building E 3.1, University, D-66123 Saarbrücken, Germany*
[7]*RSSD/SCI-SB, ESA/ESTEC, Keplerlaan 1, NL-22200AG Noordwijk, The Netherlands*
[8]*Present address: Max-Planck Institute for Extraterrestrial Physics, D-85741 Garching, Germany*
[9]*Present address: University of Cologne, I. Institute of Physics, D-50674 Köln, Germany*
[10]*Present address: GE Inspection Technologies, D-50354 Hürth, Germany*
*(*Author for correspondence: E-mail: Klaus.Seidensticker@dlr.de)*

(Received 25 April 2006; Accepted in final form 13 November 2006)

Abstract. SESAME is an instrument complex built in international co-operation and carried by the Rosetta lander Philae intended to land on comet 67P/Churyumov-Gerasimenko in 2014. The main goals of this instrument suite are to measure mechanical and electrical properties of the cometary surface and the shallow subsurface as well as of the particles emitted from the cometary surface. Most of the sensors are mounted within the six soles of the landing gear feet in order to provide good contact with or proximity to the cometary surface. The measuring principles, instrument designs, technical layout, operational concepts and the results from the first in-flight measurements are described. We conclude with comments on the consequences of the last minute change of the target comet and how to improve and to preserve the knowledge during the long-duration Rosetta mission.

Keywords: space missions, Rosetta, cometary nuclei, cometary surface, cometary particles, *in-situ* science

1. Introduction and Scientific Motivation

The primary motivation to send spacecrafts to cometary nuclei is the well-founded assumption that they are the least modified objects of the solar system since it was born out of a collapsing interstellar cloud. Thus cometary nuclei are expected to contain the primordial matter (interstellar grains made of refractory and volatile matter) and their physical properties and structure on small and large scales should give insight into the formation processes of the larger bodies 4.6 billion years ago. On the other side, one can reasonably expect that at least the surface layers

Space Science Reviews (2007) 128: 301–337
DOI: 10.1007/s11214-006-9118-6

of cometary nuclei have been modified by cosmic radiation and solar insolation, when entering the inner solar system (e.g. Belton and A'Hearn, 1999).

Sublimated ices will not only evaporate from the cometary nucleus but also will flow inward transporting energy and changing the mechanical texture of the surface layer. The bond sizes between the cometary grains would grow by condensing molecules, causing an increase of the thermal conductivity as well as of the compressive strength of the layer matrix. Prialnik and Mekler (1991) postulated that the condensation of the inward-flowing vapor will form a dense ice crust. If several ices like H_2O, CO and CO_2 were present in the primordial surface layer, their different volatility would lead to a compositional fractionation (stratification) (Benkhoff and Huebner, 1995). Each ice component would also build up its own crust at the boundary to the next upper layer. During the comet simulation (KOSI) experiments at DLR, Cologne (Seidensticker and Kochan, 1992) an initially homogeneous mixture of various ices (in most cases H_2O and CO_2) and refractory minerals developed under insolation a layered structure beneath a mm-thick dust mantle (regolith) (Grün *et al*., 1991a,b; Hesselbarth *et al*., 1991; Seiferlin *et al*., 1995).

In addition to the vertical modification of cometary surface layers, large variations of the topography over lateral scales of meters to hundreds of meters are to be expected (e.g. Belton and A'Hearn, 1999). Particles, emitted due to the sublimation of volatiles, either leave the nucleus completely or are deposited in inactive areas building up a regolith layer (Möhlmann, 1994). Thus cometary nuclei will probably show two types of surfaces areas: (i) active, bare and strong or (ii) inactive, regolith-covered and fluffy. The Stardust spacecraft to comet 81P/Wild 2 found a surface with steep slopes, even at least one overhang, suggesting a strong and cohesive surface (A'Hearn, 2004). In contrast to this observation, the Deep Impact probe transmitted data that demonstrated that comet 9P/Tempel 1 has large areas covered with smooth and loose regolith (A'Hearn *et al*., 2005).

On 2 March 2004 the lander probe Philae as part of the ESA Rosetta mission was successfully launched to comet 67P/Churyumov-Gerasimenko. Philae will land on a processed surface and the primordial state, which is hidden in the subsurface, will not be measurable directly by most of the instruments on-board. Still, the data of these instruments should improve our understanding of the processes occurring today and which have led to the present state as well as deliver essential constraints for deducing the initial composition and structure.

The Surface Electric Sounding and Acoustic Monitoring Experiment (SESAME) is part of the Philae instrument suite. SESAME is a complex of three instruments: The Comet Acoustic Surface Sounding Experiment (CASSE), the Dust Impact Monitor (DIM) and the Permittivity Probe (PP). It is the goal of SESAME to contribute to the understanding of the vertical and lateral structure of a cometary surface and the acting processes by conducting *in-situ* measurements of mechanical, electrical and particle-related properties. The analysis of elastic waves that will be generated and recorded by CASSE will allow deducing mechanical parameters as

well as the vertical (layered) structure of the cometary surface. The DIM instrument will measure the properties of impacting ice-dust grains. These data should help to improve our understanding of the lateral variations and how activity can be evoked or choked. PP will determine the complex permittivity of the surface material beneath Philae, which is a measure for the water ice content, thereby constraining the mass fractions of refractory material and other ices.

These measurements shall be performed until 67P/Churyumov-Gerasimenko reaches its perihelion. Combining observations from other instruments, both on Philae and the Rosetta orbiter, with the SESAME data should improve models of cometary activity (e.g. Möhlmann, 1995), layering processes and of the heat and gas transport within cometary surfaces.

In the following chapter we describe the physical principles behind the three instruments, their technical realization, special aspects of their operation and the expected performance. Chapter 3 gives an overview of the common central electronics and the SESAME software, which support and control the SESAME instruments. The succeeding chapters outline the operational concept of SESAME and of its instruments and present the relevant results from the Rosetta commissioning and cruise phases till March 2006. We will conclude with a discussion of the knowledge preservation aspects and of the impact of switching the target comet from 46P/Wirtanen to 67P/Churyumov-Gerasimenko on SESAME.

2. Overview of Instruments

The SESAME experiment complex consists of several sensors distributed over the Rosetta lander Philae (Figure 1), the instrument control electronics, and a common electronics, commanded via the SESAME flight software. The instruments CASSE, DIM and PP were combined during the payload selection process in order to save mass and financial resources by developing only one common electronics and one flight software. This goal was achieved to a large extent and it proved to be easier to solve the few interface problems, e.g. shielding CASSE and PP sensors of each other in the soles, within the SESAME team. The combination offers the possibility to use the data from one instrument to modify the operation parameters of another instrument within the same measurement sequence. Some of the SESAME sensors were mounted on other units of Philae that offered the advantage of a placement ("free ride") on the cometary surface. Hence SESAME did not need any transport mechanism of its own at the expense of minor interface problems.

2.1. CASSE

The outermost surface layers of cometary nuclei are evolving during every passage through the inner part of the solar system. Thus they do not show their pristine

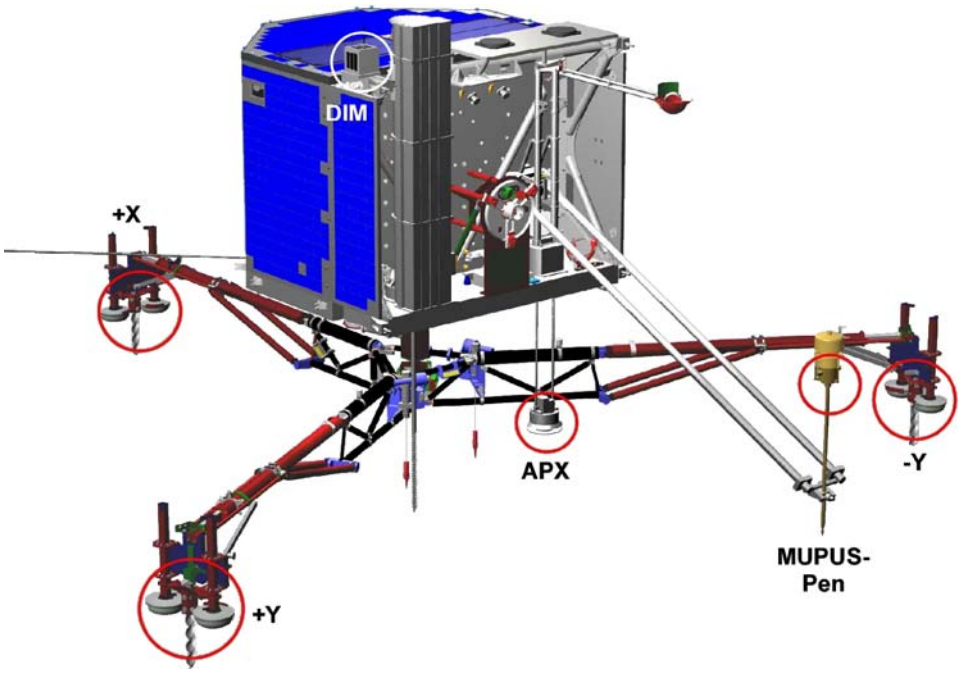

Figure 1. The Rosetta lander Philae shown in landed position with unfolded legs. The SESAME sensors are encircled and the Philae units carrying them are indicated by their designations. The feet are marked with their directional designations $+Y$, $-Y$ and $+X$.

composition and structure, but they are indicators of the cometary evolution history. Depending on the level of cometary activity (eroding the surface), the internal structure and the fraction of non-volatile matter one can expect cometary surfaces ranging from bare, sintered ice areas to thick layers of fluffy regolith. The latter kind has probably been observed on comet 9P/Tempel 1 during the crash of the Deep Impact probe (A'Hearn *et al.*, 2005). Under solar insolation, a composition of ices of different volatility will result in a stratification of the surface layer. Apart from preserving the evolution history, the surface layer determines by its parameters for heat and gas diffusion the future cometary evolution.

The Comet Acoustic Surface Sounding Experiment (CASSE) on Philae will be used to investigate the surface layers of comet 67P/Churyumov-Gerasimenko by applying active and passive methods. As CASSE can generate and register elastic and inelastic vibrations with frequencies in the range from about one hundred Hz to a few kHz, this method is called acoustic sounding because the frequencies are in the audible range. Excited elastic waves that are transmitted through the cometary matter beneath Philae and recorded by CASSE sensors allow one to detect wavefronts traveling with longitudinal and shear wave velocity. Depending on the tensile strength of the surface material and its mechanical contact to the

lander soles, we expect to study lateral and vertical elastic and structural properties of the surface layer over the foot-distance of about two meter. The primary goal of CASSE is to determine elastic parameters like Young's modulus and the Poisson ratio as well as their daily and seasonal variations by analyzing the registered signal profiles of repeated active soundings. Additional goals are:

- The monitoring of thermally or impact-caused cometary activity and the localization of activity spots;
- The determination of the macro-structure of the comet surface, such as the expected layering or embedded inhomogeneities, by using refraction and/or reflection seismograms;
- The study of emitted particles impacting on the soles during the in-orbit validation phase as well as during the descent to the cometary surface.

2.1.1. *Instrument Concept*

The Philae landing gear has three legs and feet, where each foot has two separate soles (Figure 1) with the CASSE sensors mounted into these six soles. The left sole of each foot (seen from the outside) contains the transmitter i.e. an actuator made of stacked piezoceramics that can also be operated as receiver (Figure 2). A tri-axial piezoelectric accelerometer (Brüel and Kjaer type 4506, Delta-Shear configuration with built-in pre-amplifier) mounted in the right sole is used as the primary receiver. Careful shielding with conducting Kapton foil was put in place in order to avoid

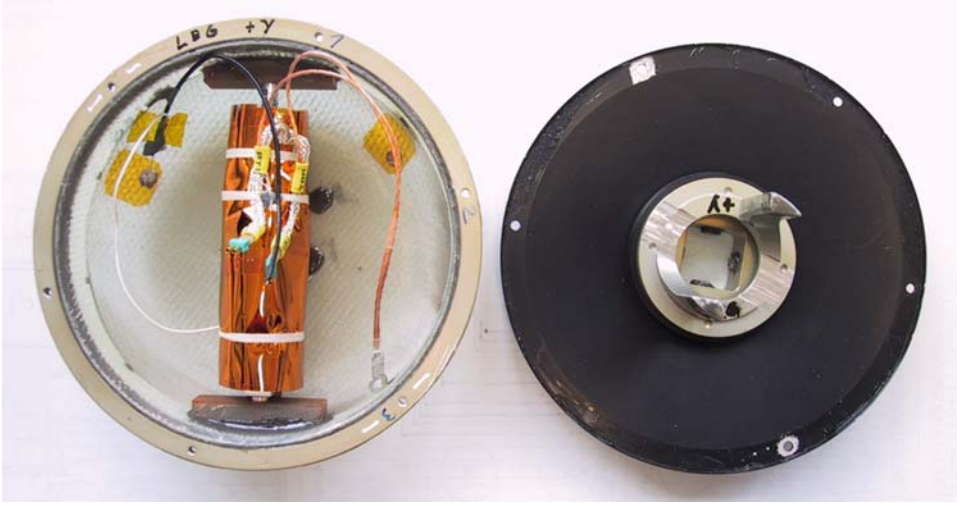

Figure 2. Photograph of the transmitter sole (left) and its black cover (right) of Philae foot $+Y$. The sole (ring diameter: 101 mm) contains an insulated wire-mesh acting as an electrode for the PP instrument. Above the mesh and between two glass-fiber bearings, the CASSE piezo-stack transmitter is mounted. The transmitter is wrapped in a conducting and grounded Kapton foil to provide shielding for PP.

any parasitic capacities from CASSE on PP and maintaining a stiff connection of the CASSE sensors with the soles. The temperature of each accelerometer and each transmitter will be measured with PT1000 thermal resistors placed below the shielding foil.

Protection struts mounted in the central part of the inner side of the lids (Figure 2) should help to avoid a breach of the glass-fiber soles during landing. A special mechanical suspension system allows the soles to adjust automatically in height by about 10 cm during landing, in order to guarantee sufficient ground contact for different surface topographies. Philae will be pulled on the comet by the two harpoons MUPUS ANC (Spohn *et al.*, this issue) providing a fixation force of at least 5 N per sole that will improve the contact between sole and cometary surface.

CASSE will measure vibrations of the foot soles in all three axes caused by elastic waves traveling through the cometary surface. In the active operation mode, the transmitters will generate pulsed elastic waves. Due to the known distances between transmitter and receiver soles and the known time of wave generation, it is possible to derive the wave-velocity. In the passive operation mode CASSE is listening to elastic waves generated either by other instruments like MUPUS PEN or by thermally or impact-caused cometary activity.

The sole contacts with the cometary surface can be considered as point-like sources. For such a point-like source, elastic wavefronts are emitted that propagate with longitudinal as well as shear wave velocities containing displacement components parallel and perpendicular to the wave-vector (e.g. Achenbach, 1973). This holds also if the wavefronts propagate along a surface. In this case an additional head wave is generated in order to maintain the boundary conditions at the surface, and as a result the wavefronts are damped. CASSE is designed to measure the arrival times of the wavefronts in order to derive the longitudinal and shear wave propagation velocities c_p and c_s and from these finally the elastic parameters Young's modulus E and Poisson ratio ν of the porous surface material:

$$E = \rho\, c_s^2 \frac{4c_s^2 - 3c_p^2}{c_s^2 - c_p^2} \tag{1}$$

and

$$\nu = \frac{c_s^2 - \frac{1}{2}c_p^2}{c_s^2 - c_p^2}, \tag{2}$$

assuming that the surface is quasi-isotropic over the scale of a wavelength (Kretschmer, 2000). A starting value for the density ρ of the material will be the global value for 67P/Churyumov-Gerasimenko determined with the orbiter instruments. The KOSI experiments showed that the density of an evolving surface layer changed by at most 20% (Hesselbarth *et al.*, 1991).

A major challenge in cometary science is to understand the phenomenon of cometary activity. Outgassing in active areas, thermal stresses between surface and

subsurface layers, and impacts of larger micrometeorites can all cause vibration signals. CASSE listening data might allow one to determine the frequency of such events at least close to Philae and to locate the epicenters of activity in cooperation with orbiter imagery.

Due to the largely unknown characteristics of the cometary surface, it is difficult to estimate the propagation environment, e.g. wavelength compared to layering dimensions. In combination with sensitivity and operation limitations of CASSE (see below) not all of the before mentioned operation modes may be possible. Thus we will check other suitable measuring modes.

In case the attenuation of the signals on the cometary surface is too large, the mechanical resonance frequencies of the soles might be exploited as well. These frequencies will change depending on the fixed force exerted by the Philae anchors, the temperature dependent stiffness of the sole glass fiber and the elastic properties of the surface matter. By modeling and calibration measurements, it should be possible to deduce elastic properties. This measuring technique has been applied for non-destructive defect detection in multilayer structures (Lange, 1994).

Operation of the CASSE sensor system like a phased array and evaluating the obtained time-series signals with an appropriate method like the Total Focusing Method (Holmes *et al*., 2005) might yield better information than comparing time series data vs. signal distance (seismogram technique) about the layered structure or the scatterers beneath Philae. However, it is presently unknown whether this operation mode is feasible considering the small number of sensors and the limited data transfer volume available.

Besides the electronics for acoustic measurements the CASSE PCB contains a radiation sensitive field-effect transistor (RadFET). It delivers a signal of the cumulated ionizing radiation dose, which can be read when the CASSE analog circuit is powered. The evaluation of the dose-signal, which is complicated by the rather complex and time-dependent composition of the radiation field, has been prepared by theoretical investigations and irradiation tests on ground (Fischer, 2002). In conjunction with the sophisticated SREM radiation monitor on the orbiter the SESAME RadFET dosimeter can be used to monitor the radiation environment of the flight electronics in-situ, which might help to improve the shielding design of future spacecraft.

2.1.2. *Performance*

Very little is known about the surface of the target comet 67P/Churyumov-Gerasimenko, neither its topography (smooth or rough) nor its configuration (chemical composition and mechanical structure). Furthermore, the sensors will experience large temperature variations, both diurnal and seasonal, that will change the sensitivity of the receivers and the transmitters as well as alter the elasticity of the foot soles.

The technical realization of CASSE was challenging, as it is the first instrument of its kind in space apart from the Apollo seismometers and the Huygens

atmospheric acoustic sensor. The foot and sole concept of Philae was changed several times during development requiring major revisions of sensor placement and integration procedures. The use of three 3-axes accelerometers as receivers and three transmitters, which can also operate as single-axis receivers, offers a lot of redundancy. In addition, the penetrator PEN of the MUPUS experiment (Spohn *et al.*, this issue) and possibly the drill mechanism SD2 (Finzi *et al.*, this issue) onboard Philae can be used as strong secondary signal sources. The operation and performance data of the CASSE sensors are given in Table I.

The attenuation within the cometary surface layer and the contact between the soles and the cometary surface, i.e. the ability to induce and to receive signals, is largely unknown. The contact with the cometary surface strongly depends on the pressure caused by the force exerted by the Philae anchors (nominally about 5 N per sole) and the elastic properties of the soles and the surface matter.

To prove that CASSE like sensors can achieve reasonable results several elastic wave propagation experiments have been conducted with various materials simulating different cometary conditions. These laboratory studies of regolithic dust and sand as well as frozen ice/dust mixtures showed that acoustic sounding can be applied to cometary surfaces as well (Kochan *et al.*, 2000; Kretschmer, 2000). Figure 3 presents sound transfer data measured with an ice-mineral sample. A sound velocity of 700 ± 60 m/s has been derived from the arrival times of the P-wave. Also visible is the strong decrease of the signal strength with distance (ca. 32 dB/m) making measurements over the Philae foot distance of 2.2 m difficult. The panels also show two other problems related to CASSE operation. Depending on sensor channel selection and receiving frequency rather large offsets of the zero line occur. If the amplification is too large, signals are cut off by the 8-bit analog-digital-converter used (see lower part of the upper profile).

TABLE I

CASSE sensors performance data

Parameter	Range	Comment
Receiving sampling rate	76.3 Hz to 100 kHz	Single channel, 1311 steps
Frequency bandwidth	3 Hz to ca. 3.3 kHz	−10 dB points of the analog electronics
Measuring range	$5.4\,10^{-3}$ to $230\,\mathrm{m\,s^{-2}}$	Tri-axes accelerometer
Temperature sensitivity of tri-axes accelerometer	0.1%/K 0.05%/K	Y and Z axes X axis
Generated frequency	1.2 Hz to 25 kHz	Depending on sampling rate and channel number
Temperature range	−160 to +100 °C	Operation range of sensors

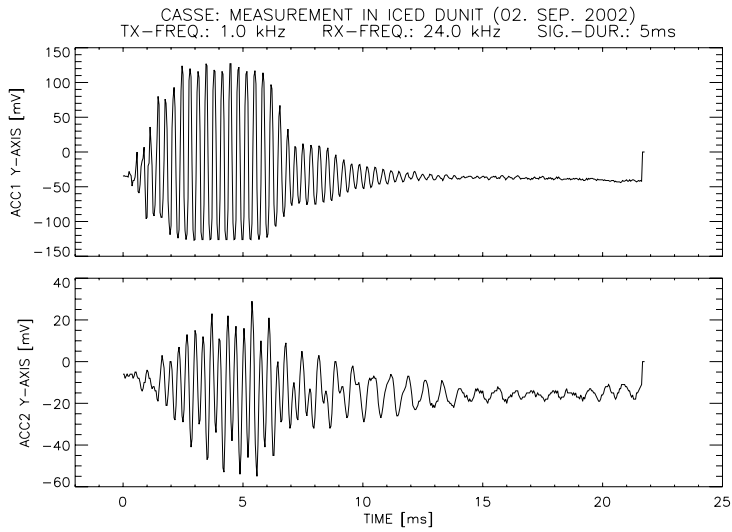

Figure 3. Sound transfer via a frozen Dunite sand bed. Laboratory models of the CASSE receiver soles were placed at distances of 40 cm (ACC1) and 80 cm (ACC2) from a CASSE transmitter sole (from Seidensticker *et al*., 2004).

Schieke (2004) supported the experimental studies and the underlying CASSE analysis by conducting numerical simulations of elastic wave propagation through porous media. These simulations suggested ways to determine the attenuation factor, and how to measure porosity and the mean pore radius of the cometary surface material from the wave velocities. The knowledge of the porosity is needed for modeling the gas flow. In addition to the experimental and numerical studies that will continue we analyze external vibrations observed during the cruise phase (see chap. 5) to improve the operation and analysis methods.

2.2. DIM

When the ice on a cometary surface is heated by solar radiation, the gas molecules released by the ice sublimation drag grains composed of refractory (dust) and volatile (ices) matter from the cometary surface. Due to the combined action of gas drag and gravitational forces grains are either ejected into space becoming part of the interplanetary dust (smaller particles) or are drawn back by gravity onto the cometary surface (larger particles). The goal of the Dust Impact Monitor (DIM) instrument of SESAME is to improve our knowledge about these particulate constituents of comets. DIM will obtain quantitative data on:

- Directional statistics of impacting particles;
- Velocity and mass distribution of back-fallen particles.

These data will be collected over an extended time period in order to find possible correlations with the cometary diurnal and orbital phases. The analysis of these data should help to:

- Improve our models of the distribution and the flux of near-surface dust and small particles as a function of their size and velocity;
- Understand cometary activity with its underlying processes;
- Explain the formation of cometary mantles.

2.2.1. *Instrument Principle*

DIM applies the principle of piezoelectricity to detect and analyze the impacting cometary particles. An impact evokes a decaying electric signal (burst), which is a mixture of several frequencies, at the output of the sensor. Nevertheless, at the beginning of this transient signal a nearly perfect half-sine wave can be observed, which lasts for the impact duration. The peak voltage is observed when the impact deformation reaches its maximum (elastic impacts are supposed). During the second quarter of the sine wave that can be a little bit deformed at the end, the particle caused deformation decreases until the grain leaves the sensor.

The method for sensing these transients is to compare them with a threshold level THR (Figure 4). This threshold is the sum of a time-average (approximately: 1 s) of the output signal of the sensor, which is equal to the noise of the electric circuit plus external noise sources, if no impacts occur, and a margin. The margin is programmable in order to adjust the sensitivity of detection. As the impact rate

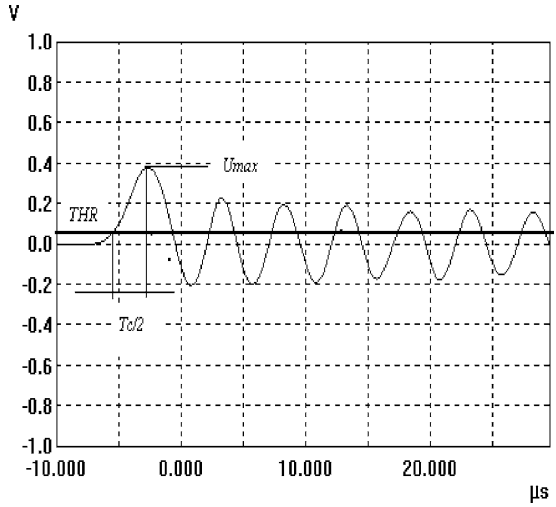

Figure 4. Typical impact signal and its measured parameters (peak amplitude $U_{\max}$ and half contact duration $T_c/2$). The parameters of the impacting particle were: mass 4 mg, velocity 0.44 m/s giving as energy 4×10^{-7} J. THR is the voltage of a threshold level.

increases, the average will increase autonomously for reducing the sensitivity so that the system will not be saturated. Events with $U_{\max} \leq$ THR will not be detected.

During a normal measurement cycle, only two parameters of the individual impact profiles are determined by the DIM electronics:

- The peak amplitude $U_{\max}$ of the first half-sine of the transient signal;
- The time between the threshold crossing and the maximum amplitude of the first half-sine $T_c/2$ (this gives the half contact duration).

DIM has two operation modes. In the Burst Continuous operation mode $U_{\max}$ and T_c are measured, but at the beginning of a measurement cycle some samples are taken from the average signal. If the background noise is very high, or the rate and/or the amplitudes of the burst signals are high, the system automatically switches to the so-called Average Continuous mode: i.e. only the average signal will be measured.

A model based on Hertz' theory describing the elastic impact of a spherical particle (e.g. Johnson, 1987) is used to relate the electric signal of the piezo-ceramic sensor to particle properties. The relationship between the voltage U of the first peak of the impact signal, yielded by the piezo-ceramic, and the radius R and the velocity v of the impacting grain can be written as:

$$U[V] = K_U(d_{33}, C, A, \rho)\ R^2\ v^{1.2} \tag{3}$$

with

$$K_U = 3.03(d_{33}/C)A^{-0.4}\ \rho^{0.6}$$

where d_{33} is the piezoelectric constant, C is the capacitance of the sensor segment and ρ is the specific mass of the impacting material. A is the reduced modulus and is given by

$$A = \left(1 - \mu_1^2\right)/E_1 + \left(1 - \mu_2^2\right)/E_2$$

where E_1, E_2 are Young's modules and μ_1, μ_2 are the Poisson ratios of the piezo segment and the grain, respectively. Likewise, the impact duration T_C is given by:

$$T_C[s] = K_T(A, \rho)\ R\ v^{-0.2} \tag{4}$$

with

$$K_T = 5.087\ A^{0.4}\ \rho^{0.4}$$

The DIM sensor (Figure 5) has three active sides each made of three piezo-plates of $50 \times 16 \times 1\,\text{mm}^3$ and facing in orthogonal directions. The other three sides of the cube are either closed by aluminum plates or are left open ($-Z$ side) for harness access. The total active area of the sensor that is mounted on Philae's balcony (Figure 1) is about $70\,\text{cm}^2$.

TABLE II
DIM performance parameters

Quantity	Range
Energy	$2{\cdot}10^{-11} - 2{\cdot}10^{-7}$ J
Mass	$6{\cdot}10^{-10} - 8{\cdot}10^{-4}$ kg
Velocity	0.025 – 0.25 m/s
Radius[a]	$5{\cdot}10^{-5} - 6{\cdot}10^{-3}$ m

[a]Spherical particles with a density of 1000 kg m^{-3} have been assumed.

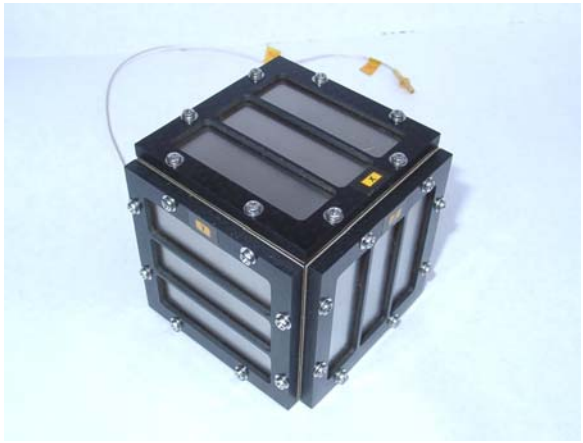

Figure 5. The DIM sensor cube with the three active piezo-plates facing to the $+X$, $+Y$ and $+Z$ directions of Philae. Overall dimensions are $71.5 \times 71.5 \times 69.0\,\text{mm}^3$.

2.2.2. *Performance*

On 2 January 2004 the NASA Stardust spacecraft crossed the coma of comet 81P/Wild 2 at a distance of 236 km with 6 km s^{-1} (A'Hearn, 2004). During this fly-through the counters of the Dust Flux Monitor Instrument (DFMI) on board Stardust recorded several thousand particles ranging in mass from 10^{-14} to 10^{-7} kg (Tuzzolino *et al.*, 2004). If this comet is representative for 67P/Churyumov-Gerasimenko, the DIM instrument is qualified to measure at least the higher mass particles of our target comet (Table II).

Drop tests were carried out, where balls of different materials and size impacted on the flight sensor. The impact velocity was calculated from the height of dropping. Figure 6 shows the correlation between calculated and measured signal amplitudes for steel balls with 1 mm diameter. Although the correlation is very good, the signal amplitudes $U_{\max}$ calculated using Equation (3) are 3 times greater than the measured ones because the elastic constants Young's modulus and Poisson ratio of the piezo plates with layers of silver and titanium could only be estimated.

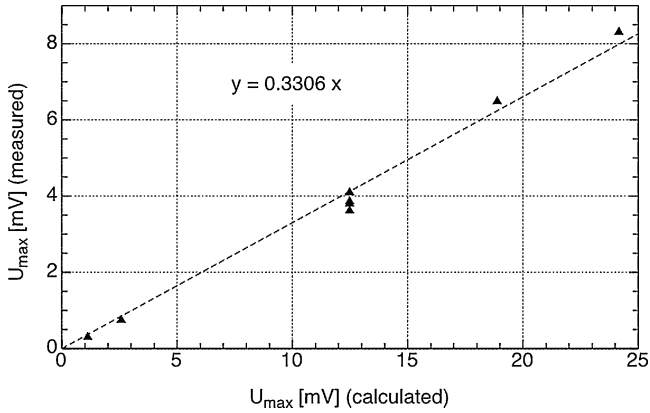

Figure 6. The correlation between calculated and measured signal amplitudes for steel balls (diameter: 1 mm) falling on the DIM flight sensor.

2.3. PP

One of the main characteristics of active comets is the ejection of large quantities of water molecules. Any water ice at the comet's surface would sublimate close to the sun due to solar irradiation leaving behind either a refractory matrix or larger dust particles. Thus the remaining ice can only be stable below the surface of active comets, where a regolith layer of unknown thickness reduces the heat influx. The depths of the ice layers and the details of the transport mechanisms of evaporated gas molecules to the surface are still unknown. As water ice dominates the electrical properties of its immediate surrounding, measuring and monitoring these properties will help to improve the understanding of gas transport and surface evolution. The aim of the Permittivity Probe (PP) instrument as part of the SESAME experiment is to determine:

- Electrical properties of the cometary surface matter and their diurnal and orbital variation
- Electron density variations close to the cometary surface as a function of the comet's outgassing activities.

The instrument measures the complex permittivity, i.e. the electrical conductivity and the dielectric polarisability of the cometary surface material. At frequencies below 10 kHz, the instrument is especially sensitive to the water ice content of the surface matter and its temperature behavior. Only the material inside the half-sphere with a radius of half the transmitter electrodes' distance contributes significantly to a measurement. As it is possible to select different electrode geometries of PP, the permittivity at different depths can be determined down to about two meters below the surface, localizing layers with different electrical properties and their

variation with time. The spatial resolution is in the order of 10% of the electrode distances.

Electrostatic and electromagnetic waves are generated by the interaction of the solar wind with the charged dust and ionized outgassing products of the comet nucleus. The resulting plasma waves can be monitored by PP in its passive operation mode with two receiver electrodes.

The measured and derived values are input parameters for an improved modeling of the properties of the cometary nucleus surface layer and the processes occurring in it. These models are a prerequisite for the interpretation of those lander- and orbiter-based experiments that aim to determine the abundances of chemical elements in the volatile primordial cometary material.

2.3.1. *Instrument Concept*

The PP instrument is based on a quadrupole array technique. Two electrodes are connected to an AC-current generator and induce a variable potential in the comet's surface, which is measured via two additional sensors (Grard, 1990a, b). The shapes of the electrodes, the configuration of the array and the location of the electrodes above or below the surface are non-critical. With an additional transmitting electrode, the geometry and thereby the observed material volume can be changed besides adding redundancy.

By injecting an alternating current of different frequencies into a medium and monitoring simultaneously the generated potential amplitudes and phase shifts between potential and current, one can deduce the dielectric properties of the medium. While for many substances the frequency dependence of the response is most pronounced in the MHz or even GHz range, water ice displays a significant variation of the permittivity at low frequencies. Below 10 kHz and at temperatures between $-80\,^{\circ}$C and $-2\,^{\circ}$C, the dielectric constant of water ice can vary by an order of magnitude. The asymptotic permittivity values for low frequencies and the frequency range of the main transition region characterize the water ice content and the temperature of the subsurface material. As this method is an integrating bulk measurement dominated by water ice, the influence of mechanical and chemical properties of other matter with small dielectric constant is below the detection level of PP.

The PP instrument generates current/voltage/phase-shift data triples corresponding to the selected measurement frequency. These data, combined with detailed knowledge of the electrodes' geometry and location, as e.g. available from Philae's CIVA stereo camera system (Bibring *et al.*, this issue), can be translated into frequency dependent complex permittivity values ε.

$$\varepsilon = \varepsilon_r - i\sigma/(\varepsilon_0\,\omega) \tag{5}$$

Here, ε_r is the relative permittivity, σ is the electrical conductivity, ε_0 is the vacuum permittivity and $\omega = 2\pi f$ is the applied angular frequency of the induced current. The relative permittivity ε_r and electrical conductivity σ can be expressed

as functions of the measured potential difference amplitudes U_0, the measured amplitudes of the injected current I_0, and the phase difference φ between current and potential by using the frequency and geometry dependent impedance Z_0. The factor G (dimension: 1/ length) takes into account the electrode geometry and thereby the measurement volume size.

$$\varepsilon_r = |2Z_0 I_0/U_0 \cos\varphi| \tag{6}$$

$$\sigma = |2\omega\varepsilon_0 Z_0 I_0/U_0 \sin\varphi| \tag{7}$$

$$Z_0 = |G/(4\pi\omega\varepsilon_0)| \tag{8}$$

$$G = 1/D_{Rx1Tx1} + 1/D_{Rx2Tx2} - 1/D_{Rx1Tx2} - 1/D_{Rx2Tx1} \tag{9}$$

Variables D_{RnTm} are the distances between the centers of receiver electrode n and transmitter electrode m. G becomes zero for a symmetrical configuration of the four electrodes, as the receiver electrodes are then placed on the same potential lines where the quadrupole arrangement is insensitive to the induced electrical field. The expression for the impedance Z_0 has been simplified by assuming point electrodes. For detailed data analysis the impedance of the actual electrodes, cables and the landing gear structure has to be modeled using a complex network modeling approach.

The two PP receiver electrode assemblies for potential difference measurements are integrated into the soles of the $+Y$ and $-Y$ landing-gear feet. Each foot includes a high-impedance pre-amplifier (Figure 7) that eliminates the impact of parasitic capacitances in harness and connectors on the measurement. An electrode in the $+X$ landing-gear foot soles is used as one of the three current transmitters. All foot electrodes consist of insulated wire meshes inside the respective soles. The electrodes and the lids of the two soles of each foot are connected by coax cables. The second transmitter electrode is integrated into the lid of the APXS detector assembly (Klingelhöfer *et al.*, this issue), the third transmitter electrode is a flexible mesh mounted at the insertion end of the MUPUS hammering device PEN (Spohn *et al.*, this issue). All electrodes are electrically insulated from their surroundings.

Changing the quadrupole array geometry by selecting either different transmitter electrode combinations or taking data with the APXS electrode placed on different surface positions after rotating Philae's body one can also derive a vertical dependence of the measured parameters, as the depth of the studied surface layer volume depends on the distance between the transmitter electrodes used.

The PP electronics is able to digitally generate any sinusoidal wave with a frequency between 10 Hz and 10 kHz and with variable peak-to-peak amplitudes up to 20 V between the two transmitter electrodes. The monitor part simultaneously acquires sample pairs of transmitter current and receiver potential differences. The current can be monitored in either of the two selected transmitter systems. An electronic switch allows connecting the two current generator poles to any two of the

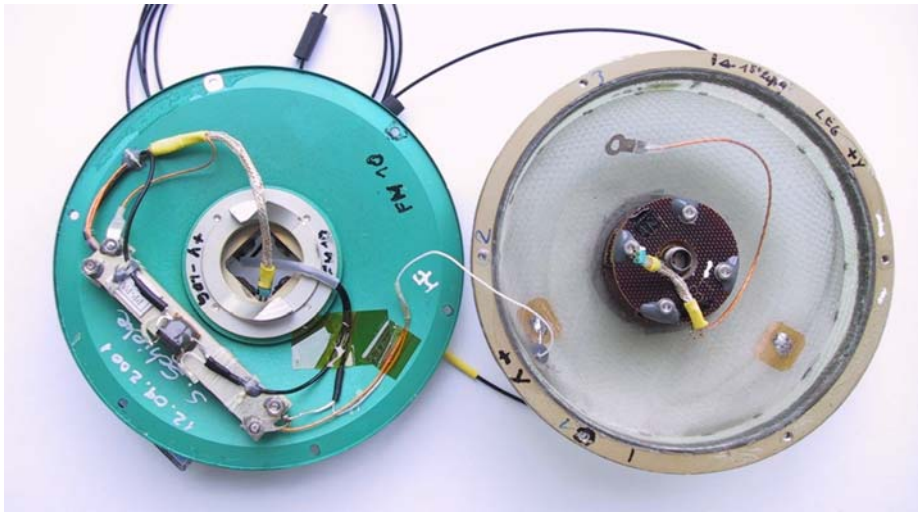

Figure 7. Accelerometer sole and cover of Philae foot $+Y$. The sole (right, ring diameter: 101 mm) contains the insulated wire mesh used as an electrode for PP and above it mounted in between two glass-fiber clamps the CASSE three-axis accelerometer. The PP pre-amplifier is mounted on the inner side of the lid (left).

three transmitter electrodes. The electrode selection determines the quadrupolar array geometry and allows selecting the subsurface volume involved in the measurement.

As the exact contact properties between comet surface material and sensor electrodes are unknown, only capacitive coupling is used. For the transmitter electrodes the exact capacitances do not matter, as the current is measured directly. For the two receiver electrodes, we measured 30.1 pF and 20.9 pF for the $+Y$ and $-Y$ feet, respectively. All electrically conductive material in the vicinity of the electrodes, including the sensor harness, is surrounded by a guarding system, which is actively kept at a potential very close to that of the electrodes but does not form a part of the measurement circuitry. This minimizes the influence of stray capacitances by 98%, which otherwise would dominate the sensor arrangement. Phase and magnitude of the measured parameters are calibrated by modeling the deployed electrode configuration on the comet and comparing the results with calibration data obtained before launch.

In the passive operation mode, when no current is injected into the comet surface, the receiver electrodes will follow the natural plasma potential at the landing gear foot positions. This will change in a characteristic way, if outgassing activities occur in Philae's vicinity. Acquiring the potential difference variations with a sampling frequency of 20 kHz and calculating the power spectrum of the resulting potential time series allows one to detect plasma waves as a consequence of such activities (Laakso *et al.*, 2002).

TABLE III
PP parameters for Active Mode operation

Parameter	Value
Transmitter frequency	10 Hz to 20 kHz, sine
Number of frequencies used	1 to 20
Maximum peak-to-peak voltage	20 V, adjustable
Phase angle resolution	1°
Current/Voltage amplitude resolution	5. . .15%, SNR-dependent

A small wire mounted close to the DIM sensor on top of Philae is operated as a plasma wave detector. This wire will pick up electrical field variations due to plasma waves, and charges a capacitor to a predefined voltage level. The faster this level is reached the larger is the AC-component of the field. The time required for reaching the detection level is reported as plasma wave detector signal and is nearly independent of the field's frequency.

2.3.2. *Performance*
While PP is not capable to determine absolute permittivity values with high accuracy, its strength lies in the possibility to monitor diurnal variations of the nucleus' behavior while the comet is approaching the Sun. The results could give a better understanding of the comet's activation mechanism. Table III summarizes the instrument's performance parameters for permittivity measurements.

Figure 8 presents a simulated potential distribution on the cometary surface during active measurements. The location of the MUPUS PEN electrode is only an example. After deployment it may be located anywhere outside the circle through the foot electrodes TX, RX1 and RX2. The exact position will be determined by using CIVA stereo-camera data. The location of the electrode at the APXS sensor will be inside the dashed line indicating the lander body.

As the measured permittivity at different frequencies depends on ice concentration, ice type, ice composition and its temperature, the resulting ambiguity can only be resolved by fitting the measured curves to reference data derived from laboratory and field measurements. Using measured local temperature and thermal conductivity data from the MUPUS sensors, the determination of water ice content can be significantly improved.

Figure 9 shows measurements of the complex permittivity as a function of frequency and temperature using a PP laboratory model (Virtanen, 2006). A sample with a sand/water ice mass ratio of 9:1 was used. Depending on the ice concentration, the low frequency values of the relative dielectric constant can vary up to 90.

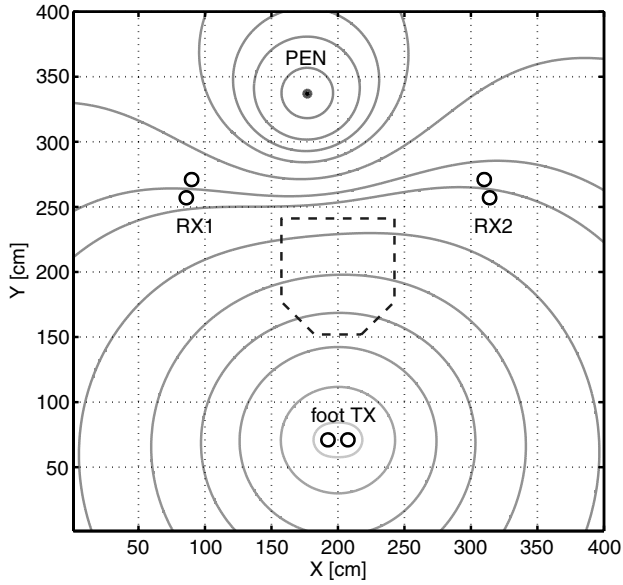

Figure 8. PP-induced simulated potential distribution on the cometary surface. The electrodes in MUPUS PEN and foot $+X$ (TX) are active. The dashed line indicates the lander body position. Simulation parameters: TX voltage 20 V_{pp}, electrode capacitances 0.85 pF (PEN) and 8.6 pF (foot TX). The resulting potential at the receiving electrodes (RX1 and RX2) is 213.6 mV_{pp} and 246.8 mV_{pp}, respectively.

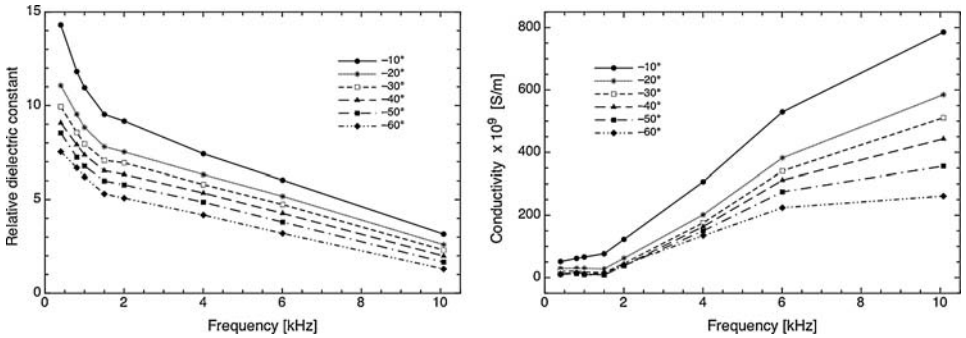

Figure 9. PP laboratory measurements on 20 February 2006 of the frequency dependence between 0.4 and 10 kHz of the relative dielectric constant (left) and the conductivity (right) of sand with 10% water ice. This dependence was measured for six temperatures from −60 °C to −10 °C (see legends).

As mentioned before, changing the quadrupole array geometry by selecting different transmitter electrode combinations or using different APXS positions one can also derive a depth dependence of the measured parameters. This capability was verified during prototype field measurements on a frozen lake in Northern

Finland in 1999 with electronics similar to that used for PP. Varying the transmitter electrode distances from 80 cm to 170 cm, we deduced an ice layer thickness of more than 60 cm and less than 75 cm. A borehole showed an actual thickness of 65 cm.

3. General Technical Layout

3.1. Central Electronics

The SESAME electronics comprises the instrument sensors, which are mounted at various locations of Philae, and the Central Electronics (CE) that is installed in the Y-EBox of the common electronic boxes inside Philae. The SESAME Central Electronics (Figure 10) itself is composed of one printed circuit board (PCB) for each of the instruments CASSE, DIM and PP and components of the common electronics that is shared by the instruments. A special PCB, the SESAME Experiment Bus, connects all boards. Power supply and data transfer to and from Philae's Command and Data Management System (CDMS) is realized with an interface board that additionally carries electronics for power management and housekeeping diagnostics. Figure 11 shows a SESAME Central Electronics stack ready for integration into the Philae electrical qualification model.

On hardware top level, each SESAME activity is controlled by a single microcomputer called Common DPU (C-DPU). It contains a radiation-hard 16-bit microcontroller (Harris RTX2010RH) with a stack-orientated multiple bus architecture. Operations on the data stack (256 words) are particularly fast and are optimized by using the programming language Forth for writing the microcontroller software. The processor instruction cycle frequency is adjusted to 5 MHz. Communication with the three instruments is managed via the processor's ASIC/Gbus, which provides 3 address and 16 data lines. Memory components of the Common DPU are a programmable read-only memory (PROM), 64 kByte electrically erasable memory (EEPROM) and static RAM (SRAM), addressed as one code page and 7 data pages with 64 kByte each. Thus a maximum of 448 kByte measurement data can be stored without data transfer to the CDMS. At system reset the boot loader ("C-DPU Debug Monitor") will be copied from PROM to SRAM and executed. By default, the SESAME flight software will be read from the EEPROM one minute later and executed. This process can be changed via dedicated telecommands to the Debug Monitor.

The Common DPU board additionally contains a 14-bit analog-digital converter, which is used to digitize the DIM peak and the average signal voltage as well as all analog housekeeping values. A Field-Programmable-Gate-Array (FPGA) provides the memory and power handling, the processor clock generation and watchdog functions. The FPGA also implements the low-level communication protocol with the CDMS.

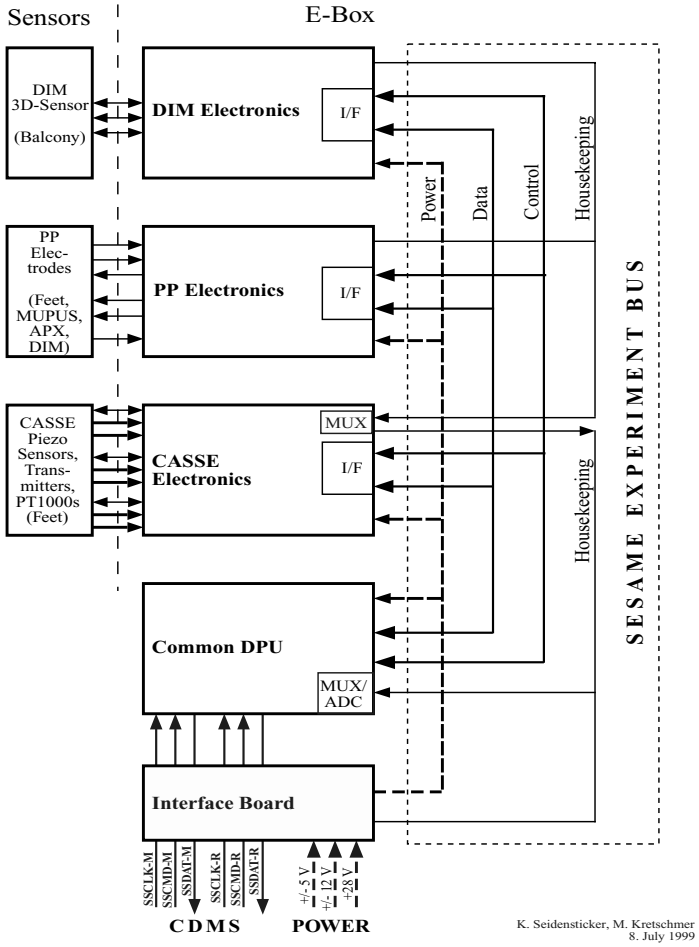

Figure 10. Block diagram of the SESAME electronics. The three boxes at left represent the SESAME sensors outside of the Philae Y-EBox. The SESAME Experiment Bus PCB ("mother board") is symbolized by the broken rectangle to the right; connection to Philae is via the Interface PCB (bottom).

3.1.1. *CASSE*

The goal of the CASSE electronics – implemented on a single PCB – was to realize a triggerable 12-channel transient recorder with a sampling rate of up to 10^5 samples/s that can be split evenly on an arbitrary number of channels. The electronics also includes a three-channel selectable signal generator with variable output frequency for the piezo-actuators. The 12 input channels are connected to the three tri-axial accelerometers and to the three piezo-actuators, which can also operate in receiver mode. The received signal coming from the input multiplexer is amplified with a selectable gain ranging from 1 to 168 (0 to 44.5 dB), converted by an 8-bit analog-to-digital converter (ADC) and continuously recorded

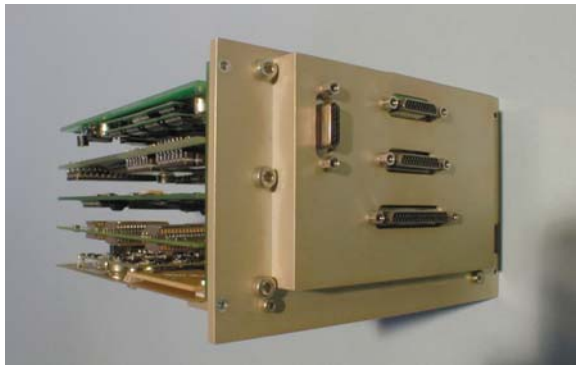

Figure 11. The SESAME electronics stack for the Philae Electrical Qualification Model. The five printed boards are (from bottom to top): Power/Interface, Common DPU, CASSE, PP and DIM. The front panel ($62 \times 100\,\mathrm{mm}^2$) has sensor connectors for CASSE, PP and DIM and a diagnostic connector (left).

in a 128 kByte ring buffer. The transfer function of the ADC is quasi-logarithmic, using piecewise linear approximation. An FPGA chip controls the data acquisition hardware, which can operate either in fixed listening mode or in triggered mode where the signal amplitude is monitored. A trigger event is generated and signaled to the C-DPU when adjustable lower or upper thresholds are crossed. Because the CASSE onboard memory is operated continuously in ring buffer mode also pre-trigger data can be captured. A recorded event is read from the CASSE memory by the flight software and further processed or handed over to the Philae CDMS for downlink.

3.1.2. *DIM*

The low-level electrical output signals of the DIM sensor pass through an analog multiplexer for selecting the direction ($+X$, $+Y$, $+Z$) of the measurement (i.e. only one direction can be measured at a time). A wideband logarithmic amplifier is used to retain the broad dynamic range of amplitudes of the input signals that are registered by an analog comparator with the help of a threshold circuit. The output of this comparator controls the peak detector and the measuring circuit for the contact duration.

All digital circuits of DIM are embedded into an FPGA, except a simple interface circuit, which is constantly powered by +5 V (even during OFF state of DIM), for the connection to the SESAME Experiment Bus. The DIM PCB contains a few additional circuits for testing its functional behavior. These circuits are used for checking the power supply voltages (±5 V), when all circuits of DIM are in ON state, the transfer characteristic of the log-amplifier, the duration (contact time) measuring circuit, and finally the sensors by

switching an electric pulse to one sensor direction at a time and measuring its response.

3.1.3. *PP*

The PP electronics consists of a sequencer implemented on a radiation hardened FPGA, a 32 kByte RAM memory and three separate analog electronics groups for transmitter sine wave generation, receiver and monitor data collection, and the wave detector, respectively. In stand-by mode, all three groups and the sequencer's clock are powered off by independent CMOS switches to conserve power. The transmitter signal is generated from a data vector stored at a fixed address range inside the RAM. According to configurable timing constraints, the values are cyclically retrieved, converted into voltages symmetrical to 0 V and fed into two of the three transmitter electrodes. This allows the generation of sine waves between 10 Hz and 20 kHz and amplitudes between 0.3 V and 20 V.

Prior to a measurement, the SESAME flight software transfers all required parameters to the PP sequencer, which will then perform the data acquisition autonomously. Data are stored in the dedicated memory and the completion of the activity is reported back to the flight software.

3.2. SESAME Software

The SESAME software consists of two different types of programs:

- The flight software is installed on the Common DPU of the SESAME lander unit. It is responsible for the autonomous (event, time tag or command controlled) sequence of measurements performed during the mission. The program code is implemented in the programming language FORTH-83 to take maximum advantage of the command structure and specific architecture of the Harris RTX2010 RH processor.
- The ground software is part of the Electrical Ground Support Equipment (EGSE) to facilitate (a) the preparation and correct formation of telecommands, parameter tables and software patches that are sent from the ground station to the lander, (b) to unpack and format the SESAME science and housekeeping data arriving at the EGSE, (c) to provide a quick-look software for data assessment, and (d) to produce files for instrument related data analysis and archiving. These tasks are presently covered by various software programs written in the programming languages TCL/TK, C++ and Delphi and will in the next few years become part of the SESAME EGSE software called AliBaba, which already covers main items of the functionality (b) and (c).

3.2.1. *Flight Software*

General concept

The main task of the SESAME flight software is to provide overall control of the scientific experiments of the instruments CASSE, DIM and PP by decoding incoming telecommands, to control and co-ordinate the various operation modes of the three instruments, to evaluate and format the SESAME science data and to organize the data flow between SESAME and the lander CDMS. Additionally, the flight software is responsible for the collection and delivery of the SESAME housekeeping data.

SESAME can be considered as a cluster experiment of three instruments with a broad range of sensors and operation modes being networked by various interdependencies. Accordingly, the SESAME control software must accommodate this complexity while satisfying a variety of quality assurance goals such as simplicity, robustness and error tolerance. These requirements are best met by a modular design of the software, which allows flexible adjustments to new operation modes and facilitates general code maintenance during the long-term mission.

Flight software architecture

The software tasks are divided into sub-tasks, which in turn are assigned to different layers (levels) or different modules of the software architecture. The SESAME flight software architecture is organized in both level and module structures (Figure 12).

Four levels may be distinguished:

- Low-level access to hardware interfaces and science experiment control;
- Communication layer, controlling telecommand and data transfer;
- Execution of telecommands and processing of science data;
- Processing of global data like Philae and SESAME status parameters as well as time and timers.

Telecommands dedicated to SESAME are generally laid down in the Stored Telecommand Buffer (STCB) of the Philae Command and Data Management System (CDMS) and will enter SESAME via the C-DPU BIOS (Basic Input Output System) and the software CDMS interface. Commands may be received without request (e.g. time-tagged) and are then passed over to the Stored Telecommand Buffer Input or may be requested by SESAME and are then directly decoded and distributed upon receipt. The telecommand decoding and distribution module checks the integrity of incoming telecommands and prepares and initiates their execution, thus acting upon the CASSE, DIM or PP measuring modules and their respective instrument hardware front ends. The Global Data and SD Output modules handle the output of global data and science data, respectively. The Housekeeping Module organizes the housekeeping data collection. The Backup RAM Buffer allows various

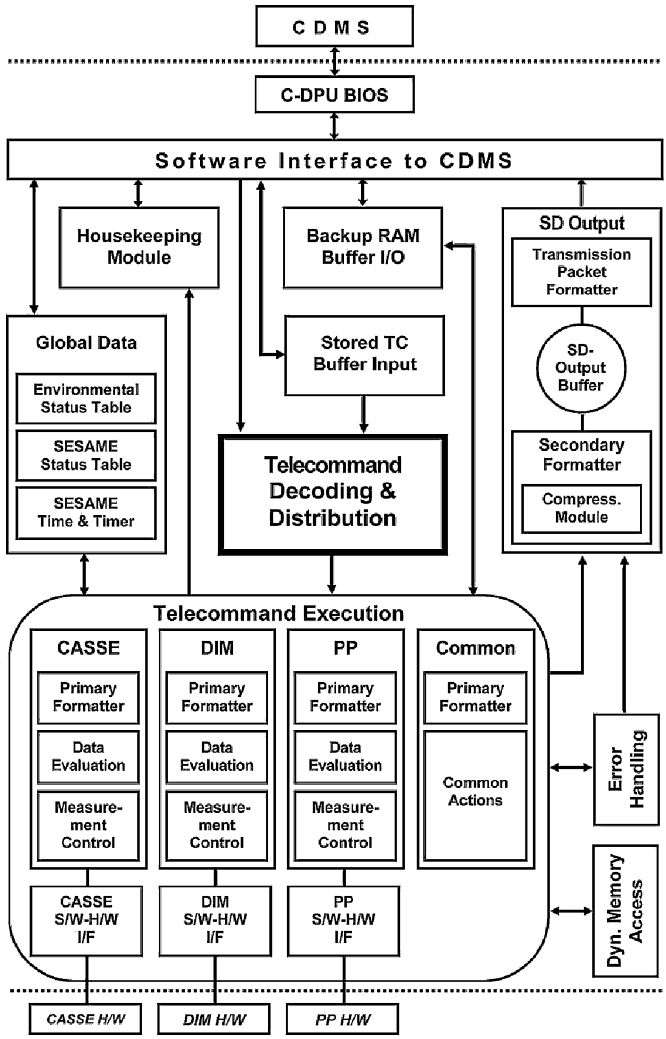

Figure 12. Architecture of SESAME flight software with main functional groups. The upper and lower dotted lines indicate the interfaces to the CDMS and SESAME hardware. There are essentially four functional groups: (1) Handling of telecommands (upper central blocks), (2) instrument control and data evaluation (lower left blocks), (3) output modules including housekeeping (upper left and right blocks), and (4) modules for memory administration and error handling (lower right).

interactions with other lander experiments. Specific routines are dedicated to error handling and dynamic access to the SESAME memory.

Implementation status

The flight software release FM 1.0, presently flying onboard of Philae provides all procedures for the autonomous control of a basic SESAME functionality. Due

to several circumstances, e.g. several changes of the Philae landing gear foot and sole design during development required a shift in man-power, we were not able to define and implement all operation modes, especially for CASSE and PP. Thus, it is planned to upgrade the flight software in future releases during the ongoing mission.

Features that will be implemented in the next release:

- New CASSE Triggered Mode for event-controlled signal registration
- Correction of CASSE FPGA program fault (missing reset) by flight software work-around
- Addition of DIM main module and minor improvements to allow autonomous DIM operation
- Revised PP algorithms for instrument settings

Features planned for flight software release FM 3 include:

- Increased autonomy of CASSE operation modes, e.g. automatic gain setting
- CASSE averaging mode for increasing the signal-to-noise ratio of weak signals
- General optimization of measuring modes based on laboratory experiments

3.2.2. *EGSE Software*

Early development of SESAME hardware and software as well as integration into Lander models was sufficiently supported by DOS routines that processed the SESAME raw data (Rosetta telemetry format) to parse them in tabular format. The transition from the development to the operational phase required a more versatile tool for a quick and intuitive check of the instrument data. Thus at the end of the year 2001 we started the development of the SESAME EGSE software, appropriately called “AliBaba”. The goals of this software program are:

- Create one tool for quick-look and validity check of SESAME science and housekeeping data generated by the lander models (FM and GRM) as well as by the SESAME EGSE.
- Provide a simple tool (graphical interface) to be used by all SESAME team members as well as other interested parties (e.g. SONC).
- Allow easy browsing on telemetry data level.
- Export data in a still to be defined format (e.g. PDS).

Since then AliBaba evolved to an indispensable tool that has been used for integration checking, development of operation procedures, and analysis of commissioning and cruise phase data.

The SESAME telemetry data packets are usually merged into one file in Rosetta Lander Binary (ROLBIN) format. This file comprises science telemetry packets, which contain measurement data of the instruments accompanied by appropriate meta-information, and housekeeping telemetry packets, which essentially provide

information on the instrument status. The first task of AliBaba is to extract all packets and rebuild the included science and housekeeping data. The meta-information (operation modes) is displayed (Figure 13) to allow the user to select data of interest.

AliBaba has been developed in Delphi (an extension of the programming language PASCAL) and runs under MS Windows 2000 and XP. All science and housekeeping data can be displayed using calibrations supporting the different hardware used in space and on the ground. A hex editor with context highlighting was implemented to dump the raw telemetry and science data for debugging purposes. The development of AliBaba continues with the main goal to support the development of our next flight software version and the checkout of the data generated with it. In addition, it is intended to enlarge the analysis methods and implement data export functions.

No.	Type	Length	UTC
1	System Message	254	07.03.2006 19:21:32
2	SESAME Healthcheck	72	07.03.2006 19:21:59
3	CASSE Sounding	11838	07.03.2006 19:22:09
4	SESAME Healthcheck	72	07.03.2006 19:23:59
5	CASSE Listening	54078	07.03.2006 19:24:19
6	CASSE Listening	8422	07.03.2006 19:27:18
7	PP Healthcheck	32	07.03.2006 19:28:44
8	PP AM Test	11798	07.03.2006 19:28:54
9	SESAME Healthcheck	72	07.03.2006 19:29:04
10	DIM Power Check	22	07.03.2006 19:29:19
11	DIM Noise Test	18	07.03.2006 19:29:19
12	DIM Calibration	76	07.03.2006 19:29:20
13	DIM Sensor Test	30	07.03.2006 19:29:22
14	DIM Sensor Test	30	07.03.2006 19:29:26
15	DIM Sensor Test	30	07.03.2006 19:29:30
16	DIM Burst Continuous	5296	07.03.2006 19:29:39
17	DIM Burst Continuous	5296	07.03.2006 19:32:29
18	DIM Burst Continuous	5298	07.03.2006 19:35:19
19	DIM Power Check	22	07.03.2006 19:38:19
20	DIM Noise Test	18	07.03.2006 19:38:19
21	DIM Calibration	76	07.03.2006 19:38:20
22	DIM Sensor Test	30	07.03.2006 19:38:22
23	DIM Sensor Test	30	07.03.2006 19:38:26
24	DIM Sensor Test	30	07.03.2006 19:38:30
25	SESAME Healthcheck	72	07.03.2006 19:38:38
26	SESAME Healthcheck	72	07.03.2006 19:38:44
27	SESAME Healthcheck	72	07.03.2006 19:38:49

Figure 13. Main window of AliBaba depicting the SESAME science operation modes (column "Type") conducted during the Philae passive checkout of 7 March 2006. The "Length" column indicates the data volume in bytes of each mode.

4. Operational Concept

Several circumstances increase the complexity of the operation of SESAME. As SESAME is a suite of three instruments one has to operate a rather large set of sensors with different physical properties. In addition, these sensors can and have to be operated in different measuring modes depending on the kind of signals one is looking for. To this end, the SESAME flight software comprises several subprograms whose parameters and settings can be changed, either by command or autonomously, to adapt the operation mode to the physical quantity or the phenomenon to be measured. One example is DIM that has to switch to a different measuring mode when single events can no longer be distinguished during high impact rates.

In order to reduce peak power consumed on Philae, to simplify programming and to diminish internal electrical interference, the three SESAME instruments are operated sequentially. However, one circuit of the CASSE electronics is continuously powered (as long as SESAME is switched on), because its multiplexer is used to register housekeeping and science data from DIM and PP (see Figure 10).

The data amount that can be transferred to Earth via the Rosetta orbiter is limited due to several circumstances: (i) many instruments and subsystems, both on Philae and the orbiter, request data transfer, (ii) the long distance to Earth (typically about 3 AU) decreases the data rate, and (iii) the radio contact duration of Philae on the cometary surface to the orbiter is rather short after the First Science Sequence (i.e. the first few days after landing). Thus the SESAME software is designed to be robust and to run quite autonomously by adapting to the measuring and storage requirements. Large data volumes will be reduced by on-board data reduction (e.g. DIM Burst Mode), averaging and lossless data compression.

Table IV gives an overview of the operation and science goals during the various phases of the Rosetta mission. Although SESAME is designed as an in-situ experiment and full operation capability requires that the landing gear is unfolded, science measurements are possible while in orbit around 67P/Churyumov-Gerasimenko. The fly-over sequences mentioned in the last line of Table IV are part of the long-term operation phase of Philae after the First Science Sequence.

Apart from planning individual SESAME operation sequences, the operation concept also has to take into account, both interferences between SESAME and other Philae units as well as the possibilities offered by common measurements. The electrical interference of SESAME on ROMAP and CONSERT was measured in May 2004 (chap. 5). In addition, CASSE and to a lesser part DIM are sensitive to mechanical disturbances as can be seen from the vibrations discovered during cruise (chap. 5). In order to quantify these effects, SESAME will be operated during planned cruise phase tests of the drill SD2 and the Philae flywheel.

TABLE IV
SESAME activities during Rosetta mission phases

Phase	SESAME	CASSE	DIM	PP
Cruise	HC*	HC	HC	HC
	S/W upgrade	Rosetta vibrations		
	EEPROM refresh			
In-Orbit	HC	HC	HC	HC
	S/W upgrade	Particle impacts?	Particle impacts	
SDL*		Particle impacts	Particle impacts	Plasma waves
		Calibration		Calibration
		Landing impact		
FSS*	HC	Elastic properties	Dust environment	Water ice amount
		Surface layer structure	Particle parameters	Plasma waves
		Cometary activity		Ice evolution
Long-term	HC	Evolution of various properties	Evolution of cometary activity	Evolution of cometary activity
				Plasma waves
Fly-over sequences[a]		Ground truth	Ground truth	Ground truth
		Localization of cometary activity	Particle flow	Plasma wave evolution

*Abbreviations: HC: Health-check; S/W: Software; SDL: Separation, Descent and Landing; FSS: First Science Sequence.
[a]Common operation with Rosetta orbiter experiments.

The possibilities of co-operation with other Philae experiments have been taken into account since the beginning of the SESAME operation planning. Apart from the simple off-line sharing of data obtained by different instruments, e.g. ROMAP and PP, and the planning of more sophisticated common operation during so-called fly-over sequences (see Table IV), we are planning for detailed information interchange on board via the CDMS Backup RAM to adapt operation autonomously to the actual status. The data interfaces with the instruments SD2 and MUPUS have already been agreed. The insertion (hammering) of the MUPUS PEN should generate a strong sound signal that can be used by parallel CASSE measurements depending on the actual PEN depth to determine the cometary surface structure. On the other hand, PP can only operate actively when the MUPUS PEN is inserted, but not operating. This information is accessible to SESAME via the CDMS backup RAM buffer of MUPUS.

4.1. CASSE

The operation of the CASSE instrument can be divided into three basic modes:

- Sounding mode: a transmitter generates a signal that can be registered by any CASSE receiver (3-axis accelerometer or another transmitter)
- Listening mode: the selected receiver registers immediately any signal for a predefined duration
- Triggered mode: like the listening mode, but signals are processed only if a predefined threshold is exceeded.

These basic modes have been and will be used to develop secondary operation modes. Examples are the on-board averaging of several sounding time series in order to improve the signal-to-noise ratio and the automatic selection of the amplifier gain in order to optimize the dynamic range of the analog-digital-converter (ADC). One of the more elaborate operation modes will run during the insertion of MUPUS PEN into the cometary surface, as the measurement rate has to depend on the insertion speed.

The operation of CASSE hardware and the data analysis have to take several limitations into account. CASSE had to use a space qualified 8-bit ADC. In order to enlarge the dynamic range the ADC transfer function is quasi-logarithmic increasing the range by a factor of 2 at the expense of a decreased resolution. In addition, several amplification factors between 1 and 168 (0 to 44.5 dB) can be selected. During the simultaneous operation of several receivers the CASSE electronic generates a channel-dependent DC-offset (Fischer, 2002) that limits the combination of receivers as otherwise the dynamic range would become too small. Finally, the sensitivity of the tri-axial accelerometers decreases by about 0.05 to 0.1%/K (depending on the axis used) in the temperature range from $+100\,^{\circ}$C to $-160\,^{\circ}$C (Fischer, 2002). The temperatures of all CASSE sensors are monitored to correct these sensitivity changes during analysis. In order to reduce the impact of these effects on the scientific results, emphasis is on the analysis of relative data. Thus we intend to measure time differences (wave velocities) and to use the signal profile for sound propagation modeling.

It is intended to use the cruise phase to check and to improve the pre-launch calibration data by conducting calibration measurements both with the flight and laboratory hardware. CASSE data are not only affected by the instrument design but also by external effects. These are Philae internal noise sources (e.g. fly-wheel operation during descent and landing) as well as sound transfer via the landing gear (on comet). It is therefore planned to determine the sound transfer through the unfolded landing gear during the descent.

4.2. DIM

During each operation of DIM, the average value of the amplified signal is sampled. In case of low impact rates, this is roughly equivalent to the sum of electronic and background noise. For very high impact rates, the individual impacts can no longer be distinguished so only the average value of the signal is measured. The

switchover from measuring individual impacts (Burst Continuous mode) to the average (Average Continuous mode) is performed by the flight software, based on the measured mean. However, this autonomous decision-making can be disabled by telecommands.

The flight software controls the measurement (start/stop, mode selection etc.), data storage and compression, but does not calculate the velocities or radii of impacting particles. The flight software samples the compressed data containing peak amplitudes, half contact times and mean values and transmits them to Earth via the Philae CDMS.

4.3. PP

The data obtained in active mode consist of averaged and preprocessed numbers for the measurement configuration, transmitter frequency, transmitter current, receiver voltage, and receiver voltage phase-difference with respect to the measured current signal. Each measurement includes about ten different frequencies in the range of 60 Hz to 10 kHz for three different amplitudes. Different amplitudes are necessary to increase the dynamic range for small signals from low temperature/low water ice content to large signals in case of larger amounts of water ice at higher temperatures.

During PP's passive mode operation the power spectrum is calculated from the potential difference time series, sampled with 20 kHz, by means of a simplified wavelet algorithm, which provides logarithmically-binned power-spectrum information above 10 kHz, 5 kHz etc. The plasma wave monitor requires the smallest amount of resources in terms of power and telemetry. It is therefore read out whenever SESAME is powered on. The sensor value is included in the housekeeping data stream and might indicate surface activity also during times when the rest of the PP instrument is not operating. This value is a measure of the integrated power of the spectrum and indicates if real plasma wave activities are present.

Data from active measurements obtained during the descent after the foldout of the landing gear are reference values for the vacuum conditions (relative permittivity $= 1$, conductivity $= 0$) and are essential for the final data analysis and calibration. However, due to differences in the instrument configuration (MUPUS PEN not deployed, APXS not deployed) the data will have to be corrected using results from laboratory tests and from the flight model calibration campaign.

The positions of the PP transmitter electrodes on APXS and MUPUS PEN are dependent on the activities of these experiments. The active mode configuration including the MUPUS PEN with its permanently fixed deployment will offer the possibility of long-term studies under otherwise identical conditions, while the APXS detector may be positioned under different lander rotation angles, offering different geometries and signal penetration depths.

5. Results from the Commissioning and Cruise Phases

The commissioning phase of the Rosetta mission in 2004 was used to check the status of SESAME. As the SESAME instruments prior to landing on the target comet do not have their full functionality in space (e.g. the landing gear has to be unfolded for allowing all PP operation modes) only a subset of operation modes could be tested. With these limitations in mind, the SESAME commissioning operations had the following goals:

- Verify that all sensors and the central electronics are operational in accordance with the design specifications;
- Test the flight software, the communication with the Philae CDMS, and the operational procedures;
- Check the impact of Philae operating configuration, i.e. power converter mode and different temperatures of the Y-EBox (a Philae electronics container), on SESAME;
- Measure the interference of SESAME on ROMAP and CONSERT.

In the course of the commissioning phase and the subsequent cruise phase, SESAME flight procedures have been modified and extended, whenever this effort seemed to be justified by new questions or interesting measuring results. The actual SESAME command sequence "Cruise Functional Test" for instance, includes listening modes for CASSE and DIM in order to search for external disturbances.

5.1. Instrument Status

All measurements have indicated that the SESAME instruments are healthy and work as expected. There is a minor problem with the CMDS communication that is currently being solved by sending three health-check commands to SESAME at the end of each command sequence in order to force the transmission of all measurement data to the CDMS (see Figure 13).

The impact of different Philae operating configurations on SESAME data is negligible. Calibration data like the characteristics of the DIM logarithmic amplifier or electronic noise are gathered for different operating conditions (e.g. low and high temperatures of the central electronics). Their evolution with time will be observed until landing.

The performance of CASSE was as expected delivering reproducible signals. Due to a missing reset in the FPGA code, a few time series data are either lost or the sample positions are shifted. Depending on the setting of various parameters, e.g. transmitting and receiving frequencies, some signals exhibit shifts from the zero line (offsets, see Figure 3) that reduce the dynamic range. It is one goal of the on-going calibration effort to find better telecommand parameters.

The electronic noise measured by DIM is quite high, ranging between 30 and 40 dB, but acceptable. Assumed sources are either the lander CDMS or the power converters, which are located next to the SESAME central electronics in the Philae Y-EBox. Until now, the DIM instrument did not detect any impacts. Apart from the scarcity of particles in space, the short operation duration and the mounting of Philae on the backside of the Rosetta orbiter cause this result.

PP health-checks also showed no problems. The pre-amplifiers located in the landing gear feet were optimally balanced during all test blocks. Plasma wave activities could not be observed during the few seconds when those measurements were performed. Active mode tests are not possible with the landing gear legs folded to the Philae body.

5.2. Interference Tests

On request of the ROMAP and CONSERT teams interference tests with other Philae experiments, including SESAME, have been performed during the commissioning period in May 2004. The ROMAP magnetometer data trace almost exactly the SESAME power consumption (like that of the other instruments). This indicates

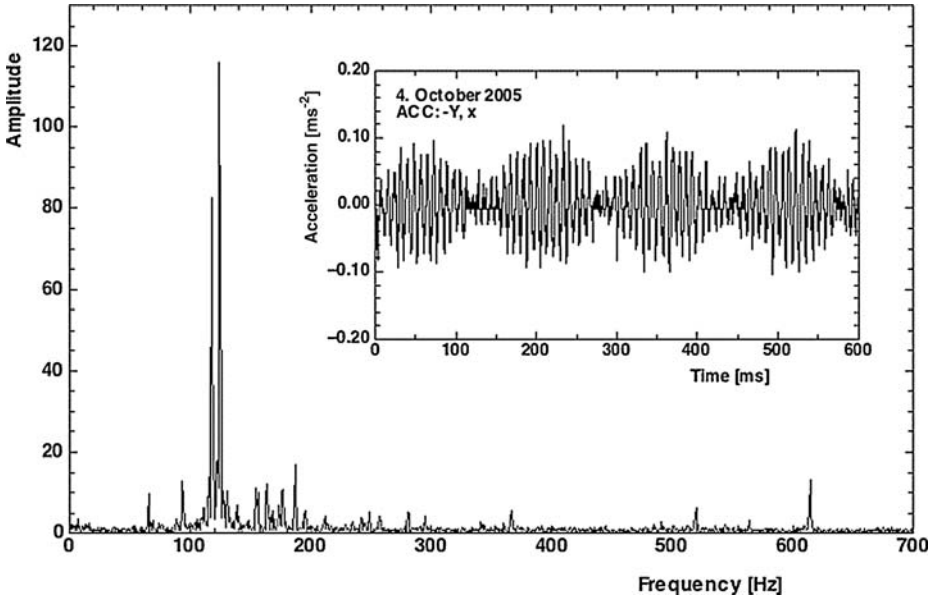

Figure 14. Frequency spectrum of CASSE accelerometer data (foot $-Y$, x-axis) measured in passive (listening) mode during Philae Checkout #1 (4 October 2005). There are no contributions to the signal above 700 Hz. The insert shows the first part of the signal time series (total duration: 1000 ms). Due to the strong vibrations with 117.7 and 124.3 Hz a beat is clearly visible in the signal.

that the source of magnetic disturbance is not the operation of the instruments itself but a current loop in the power supply. This shall be further investigated by another test, operating Philae by using the power of its secondary battery and not – as usually during cruise – the orbiter power via an umbilical line. CONSERT measurements are also disturbed when SESAME is active. In addition to the ground loop effect mentioned above, there is excess noise during the short periods when the SESAME instruments are actually measuring (including housekeeping data acquisition). As a consequence the housekeeping data sampling frequency will be decreased in the next version of the SESAME flight software.

5.3. Vibrations

CASSE listening measurements have been included in the SESAME operation sequence in order to investigate yet unexplained vibrations of the lander soles discovered during the commissioning phase. These micro-vibrations (amplitudes below $0.1\,\mathrm{ms}^{-2}$) occur mainly with frequencies in the range from 60 to 200 Hz. Figure 14 presents an amplitude frequency spectrum obtained by a fast Fourier transform of a measurement (insert) conducted on 4 October 2005. The acceleration has been calculated by applying pre-launch calibrations for the analog-digital converter, amplifier and the accelerometer. The slight decrease in sensitivity due to the lower temperature has not been corrected. The signal period with 6.7 Hz (insert of Figure 14) is a beat caused by the interference of the two strong vibrations with frequencies of 117.7 and 124.3 Hz. Although we cannot exclude that the vibrations are caused by CASSE as the listening is conducted after a sounding measurement (see Figure 13), the most likely explanation is an external source, probably the orbiter reaction wheels. The observed vibration will be investigated with modified operation sequences during forthcoming Philae checkouts.

5.4. Temperatures

Table V lists representative temperature data measured on the accelerometers mounted in the Philae feet ($+Y$ and $-Y$) facing the orbiter as well as on the CASSE PCB inside Philae. For most dates, the temperature variation during the measurement sequences lasting less than 30 min is given. The mean temperatures depend on the location of the sole (the temperature of foot $+X$ was always below $-104.5\,^{\circ}\mathrm{C}$, the measuring limit), the S/C attitude and the solar distance. The temperatures increase during CASSE measurements, particularly the accelerometer temperatures due to the operation of the pre-amplifiers. Taking into account the different locations of the external and internal temperature sensors, the SESAME temperature data compare well with reference data delivered by Philae's thermal control unit (TCU).

TABLE V
Selected SESAME temperature data[a]

Date	T (CAS-PCB) [°C]	T (ACC $+Y$) [°C]	T (ACC $-Y$) [°C]
2004 Mar. 17	$+21.4 \cdots +23.0$	-97.1	-97.2
2004 Apr.14	$+40.2 \cdots +42.2$	-91.0	-91.8
2004 May 15	$-14.1 \cdots -7.7$	$-98.6 \cdots -96.0$	$-96.1 \cdots -93.5$
2004 May 20	$-9.1 \cdots -2.3$	$-97.5 \cdots -95.6$	$-94.8 \cdots -93.0$
2004 Oct. 6	$+6.8 \cdots +12.4$	$-100.9 \cdots -99.0$	$-100.9 \cdots -99.1$
2005 Mar. 29	$-24.8 \cdots -20.5$	$-104.0 \cdots -100.2$	$\leq -104.5 \cdots -103.1$
2005 Oct. 4	$-28.9 \cdots -24.3$	≤ -104.5	≤ -104.5
2006 Mar. 7	$-18.0 \cdots -14.0$	≤ -104.5	≤ -104.5

[a]For the longer measurement sequences, the temperatures at the beginning and the end of each period are given, indicating the heat released by the PCB and the sensors. Temperatures on foot $+X$ (mounted away from the orbiter) were always ≤ -104.5 °C. The lower measuring limit of -104.5 °C is caused by a mistake made during the manufacturing of the CASSE electronics.

6. Summary and Conclusions

The analysis of the various in-flight tests during the Rosetta commissioning phase and the following cruise phase confirmed that all SESAME instruments and the common electronics are functional and work as expected. However, the present version of the flight software does not use the full operational functionality of the hardware. This is a consequence of a pre-launch decision, to use most of the manpower available for finishing the hardware in time. Thus, it is intended to improve the implemented operation modes and to add new ones in future upgrades of the flight software.

More sophisticated operation modes, especially for CASSE, need to be tested and calibrated in ground-based experiments before being implemented. For the interpretation of the complex acoustic sounding and listening data of the CASSE instrument the development of numerical models is required. Details of the SESAME operation modes in general have to be improved in conjunction with theoretical modeling to retrieve the optimum scientific impact from the collected data.

The short-term switching of the Rosetta target comet (from 46P/Wirtanen to 67P/Churyumov-Gerasimenko) and the resulting change of primary physical parameters requires operation and software modifications and may influence the scientific output of SESAME (Seidensticker *et al.*, 2004). The larger mass of the new target comet via stronger gravitation considerably shortens the separation, descent and landing phase (SDL) of Philae. This phase is essential for SESAME both

for calibration purposes and for obtaining non-recurring data, e.g. particle number density vs. height. Increased dust emission could affect both, Philae and DIM in particular. Kidger (2003) reported that during the 2002–2003 apparition comet 67P/Churyumov-Gerasimenko experienced a large outburst at perihelion where the dust production rate doubled. Similar observations were made at previous perihelion passages. The higher touch-down velocity up to $1.5\,\mathrm{ms}^{-1}$ compared to the $0.5\,\mathrm{ms}^{-1}$ landing speed of 46P/Wirtanen increases at least the risk of loosening the CASSE or PP sensor fixations within the soles.

In view of the decade-long Rosetta mission duration knowledge preservation and knowledge transfer turns out to be an important factor. Changes of the SESAME team membership with time as well as revisions in data storage techniques like data format and storing devices require continuing specific measures and procedures of data archiving. In cooperation with SONC the transfer and storage of data and documents in a standard format like that of the Planetary Data System (PDS) at an ESA archive site is planned.

The present paper is meant as an overview introducing the principal scientific objectives of SESAME, the technical design of the instruments, and the operational concept to achieve these objectives. Forthcoming papers will be dedicated more specifically to the SESAME instruments CASSE, DIM and PP dealing in greater detail with their measurement algorithms, calibration procedures, and laboratory results.

Acknowledgements

The delivery of the SESAME instrument would certainly not have been achieved in time without the invaluable assistance of a variety of individuals and organizations:

The Common DPU that is a major constituent of the SESAME Central Electronics (CE), influencing also the design of the SESAME Flight Software, has been developed and built by R. Schrödter and A. Lichopoj, both from DLR, Berlin. H. von Hoerner and L. Ziegler at von Hoerner & Sulger GmbH, Schwetzingen, Germany, developed the concept of central electronics as the hardware cornerstone of SESAME. L. Ziegler and G. Krein (von Hoerner & Sulger GmbH) built the CASSE PCB, the SESAME experiment bus, tested all delivered PCB and integrated the various stacks of the central electronics. W. Gebhardt and R. Licht (both from FHG-IZFP, Saarbrücken, Germany) designed, built and tested the piezo-electric stacks (transmitter) required for CASSE sound generation in the Philae soles. H. Rosenbauer and B. Chares (both from MPS, Lindau/Harz, Germany) took great care to comply with the experimental requirements of CASSE and PP when designing and building the Philae feet and soles. B. Johlander and B. Butler (both from ESTEC, The Netherlands) supported considerably the integration of the CASSE and PP sensors in the soles and into the Philae feet. The authors also wish to thank P. Penkert (DLR, Cologne, Germany) for his support during harness design and manufacturing, R. Enge (MPS, Lindau, Germany) for building the interface PCB,

and K.-V. Rehmann as well as T. Tokano (both DLR, Cologne, Germany) for conducting the incoming inspections. We thank the Lander Team for its continuing support and patience during design, integration and development and execution of operational procedures. The comments by the reviewers greatly helped to improve this paper.

Both institutional funding and special grants or contracts have supported the development of SESAME and its instruments:

SESAME and CASSE have been supported by DLR and by the former German space-funding agency DARA. D. Möhlmann gratefully acknowledges DARA contract FKZ 50 QP 9707 for SESAME and CASSE development; K. Thiel wishes to thank for the financial support of DARA and DLR under contract 50QP9719 for software development and the FHG-IZFP gratefully acknowledges grant 01QP9720 of DARA used for designing and building the CASSE piezo-actuators.

The PP instrument development has been supported by grants from the Finnish Academy of Science and Letters and the Center for Technical Development TEKES. The practical support by ESTEC/SSD for PP integration and by the Rosetta APXS and MUPUS teams for the development and integration of PP sensors on their instruments is gratefully acknowledged. The DIM development has been supported by the Hungarian Space Office via the ECS organization of ESA and the KFKI Atomic Energy Research Institute of the Hungarian Academy of Sciences. Many thanks are also due to the Max Planck Institute for Solar System Research, Lindau, Germany, for its continuous technical support.

References

A'Hearn, M. F., Belton, M. J. S., Delamere, W. A., Kissel, J., Klaasen, K. P., McFadden, L. A., *et al.*: 2005, *Science* **310**, 258.

A'Hearn, M. F.: 2004, *Nature* **429**, 818.

Achenbach, J. D.: 1973, *Wave Propagation in Elastic Solids*, North-Holland Publishing Company, Amsterdam, London, p. 425.

Belton, M. J. S., and A'Hearn, M. F.: 1999, *Adv. Space Res.* **24**, 1167.

Benkhoff, J., and Huebner, W. F.: 1995, *Icarus* **114**, 348.

Bibring, J.-P., Lamy, P., Langevin, Y., Soufflot, A., Berthé, M., Borg, J., *et al.*: *Space Sci. Rev.* this issue, doi: 10.1007/s11214-006-9135-5.

Finzi, A. E., Magnani, P. G., Re, E., Espinasse, S., and Olivieri, A.: *Space Sci. Rev.* this issue, doi: 10.1007/s11214-006-9134-6.

Fischer, H.-H.: 2002, 'Software-Entwicklung für das SESAME-Experiment der Rosetta-Kometenmission und Untersuchungen zum RadFET-Dosimeter', PhD thesis, Universität zu Köln, p. 141.

Grard, R.: 1990a, *Meas. Sci. Technol.* **1**, 295.

Grard, R.: 1990b, *Meas. Sci. Technol.* **1**, 801.

Grün, E., Bar-Nun, A., Benkhoff, J., Bischoff, A., Düren, H., Hellmann, H., *et al.*: 1991a, In: R. L. Newburn Jr., M. Neugebauer, and J. Rahe (eds.), *Comets in the Post-Halley Era*, **1**, Kluwer Academic Publishers, 277.

Grün, E., Kochan, H., and Seidensticker, K. J.: 1991b, *Geophys. Res. Let.* **18**, 245.

Hesselbarth, P., Krankowsky, D., Lämmerzahl, P., Winkler, A., and Mauersberger, K.: 1991, *Geophys. Res. Let.* **18**, 269.

Holmes, C., Drinkwater, B. W., and Wilcox, P. D.: 2005, In: D. O. Thompson and D. E. Chimenti (eds.), *Review of Progress in Quantitative Nondestructive Evaluation* **24**, 946.

Johnson, K. L.: 1987, *Contact Mechanics*, Cambridge University Press, p. 464.

Kidger, M. R.: 2003, *Astron. Astrophys.* **408**, 767.

Klingelhöfer, G., Brückner, J., d'Uston, C., Gellert, R., and Rieder, R.: *Space Sci. Rev.* this issue, doi: 10.1007/s11214-006-9137-3.

Kochan, H., Feibig, W., Konopka, U., Kretschmer, M., Möhlmann, D., Seidensticker, K. J., *et al.*: 2000, *Planet. Space Sci.* **48**, 385.

Kretschmer, M.: 2000, 'Schallausbreitung in Kometen-relevantem Material', PhD Thesis, Universität zu Köln, p. 128.

Laakso, H., Grard, R., Janhunen, P., and Trotignon, J.-G.: 2002, *Ann. Geophys.* **20**, 1.

Lange, Y. V.: 1994, *Nondestructive Testing and Evaluation* **11**, 177.

Möhlmann, D.: 1994, *Planet. Space Sci.* **42**, 933.

Möhlmann, D.: 1995, *Planet. Space Sci.* **43**, 327.

Prialnik, D., and Mekler, Y.: 1991, *Astrophys. J.* **366**, 318.

Schieke, S.: 2004, 'Beiträge zur Numerischen Simulation des Instrumentes CASSE der ESA-Mission Rosetta', PhD thesis, Universität des Saarlandes, p. 134.

Seidensticker, K. J., and Kochan, H.: 1992, *Ann. Geophys.* **10**, 198.

Seidensticker, K. J., Fischer, H.-H., Madlener, D., Schieke, S., Thiel, K., Péter, A., *et al.*: 2004, In: L. Colangeli, E. M. Epifani, and P. Palumbo (eds.), *The New Rosetta Targets – Observations, Simulations and Instrument Performances*, Astrophysics and Space Science Library **311**, Kluwer Academic Publishers, 297.

Seiferlin, K., Spohn, T., and Benkhoff, J.: 1995, *Adv. Space Res.* **15**, 35.

Spohn, T., Seiferlin, K., Hagermann, A., Knollenberg, J., Ball, A. J., Banaszkiewicz, M., *et al.*: *Space Sci. Rev.* this issue, doi: 10.1007/s11214-006-9081-2.

Tuzzolino, A. J., Economou, T. E., Clark, B. C., Tsou, P., Brownlee, D. E., Green, S. F., *et al.*: 2004, *Science* **304**, 1776.

Virtanen, J.: 2006, 'Theory and Praxis of the Permittivity Probe Quadrupole Measurements', Diploma Thesis, University of Helsinki, p. 105.